Frontiers in Bioscience Landmark

Front. Biosci. (Landmark Ed) **2026**; 31(9): 52847
https://doi.org/10.31083/FBL52847

Original Research

SRPK Inhibition in Cholangiocarcinoma Cells Induces LAMB1-Associated Adaptive Responses and Enhances Growth Suppression by the MEK Inhibitor U0126 via the LAMB1/ERK/c-JUN Axis

Chaturong Inpad[1], Prakasit Khamsuwan[1], Phuwapat Vongkaewpothong[1], Waritsara Susena[1], Kanyanut Kotanart[1], Tavan Janvilisri[2], Hathaichanok Impheng[3], Atit Silsirivanit[4], Sittiruk Roytrakul[5], Worasak Kaewkong[1,*]

[1]Department of Biochemistry, Faculty of Medical Science, Naresuan University, 65000 Phitsanulok, Thailand
[2]Department of Microbiology, Faculty of Science, Chulalongkorn University, 10330 Bangkok, Thailand
[3]Department of Physiology, Faculty of Medical Science, Naresuan University, 65000 Phitsanulok, Thailand
[4]Department of Biochemistry, Faculty of Medicine, Khon Kaen University, 40002 Khon Kaen, Thailand
[5]National Center for Genetic Engineering and Biotechnology, National Science and Technology Development Agency, 12120 Pathum Thani, Thailand
*Correspondence: worasakk@nu.ac.th (Worasak Kaewkong)

Academic Editor: Amancio Carnero Moya
Submitted: 13 April 2026 Revised: 8 August 2026 Accepted: 18 August 2026 Published: 7 September 2026

Abstract

Background: Cholangiocarcinoma (CCA) is an aggressive bile duct malignancy with a high incidence and mortality rate in Southeast Asia, particularly in Thailand. However, current treatments offer only limited clinical benefit. Aberrant mRNA splicing, driven by hyperactivation of serine/arginine-rich splicing factors (SRSFs) and their upstream kinases SRPK1 and SRPK2, contributes to the progression of CCA. Although SRPK inhibitors suppress tumor growth, their effects remain incomplete, highlighting the need for rational combination strategies. **Methods:** Liquid chromatography–tandem mass spectrometry (LC-MS/MS)-based proteomic profiling was performed on CCA cell lines (KKU-213A and KKU-055) treated with the SRPK inhibitors SRPIN340 and SPHINX31. Subsequently, commonly upregulated differentially expressed proteins (UpDEPs) were identified and cross-validated with data from the Cancer Genome Atlas (TCGA) using GEPIA, followed by reverse transcription-quantitative polymerase chain reaction (qRT-qPCR) validation. The functional effects of combined SRPK and mitogen-activated protein kinase kinase (MEK) inhibition (with U0126) were evaluated using cell viability and colony formation assays, and by analyzing signaling pathways. **Results:** A total of 34 common UpDEPs were identified following SRPK inhibition. Laminin subunit beta 1 (LAMB1) was prioritized as a candidate combination target due to robust upregulation, concordant overexpression in TCGA datasets, and increased mRNA levels after SRPK inhibitor treatment. Given prior evidence linking MEK signaling to LAMB1 regulation, we also evaluated the MEK inhibitor U0126. Combined treatment with SRPK inhibitors (SRPIN340 or SPHINX31) and U0126 produced greater suppression of viability and clonogenic growth in KKU-213A cells than either treatment alone. These effects were accompanied by reduced ERK phosphorylation and cellular Jun proto-oncogene (c-JUN) expression. **Conclusions:** LAMB1 represents a potential adaptive response target following SRPK inhibition in CCA. Dual targeting of SRPK and MEK signaling pathways exerts greater antitumor effects than either treatment alone and may provide a promising therapeutic strategy for CCA management.

Keywords: alternative splicing; cholangiocarcinoma; laminin beta 1; proteomics; serine-arginine protein kinases

1. Introduction

Cholangiocarcinoma (CCA) is an aggressive epithelial malignancy originating from the biliary tract and is anatomically classified into intrahepatic, perihilar, and distal subtypes, with further categorization based on tumor growth patterns [1]. The incidence of CCA is disproportionately high in Southeast Asia, particularly in Thailand, where a major etiological factor is chronic infection with hepatobiliary flukes such as *Opisthorchis viverrini* [2]. Additional risk factors include primary sclerosing cholangitis, choledochal cysts, hepatolithiasis, chronic viral hepatitis, cirrhosis, and exposure to environmental carcinogens [1]. CCAs are highly heterogeneous from the clinical, histomorphological, and molecular perspectives but often share a poor prognosis [3]. Despite the availability of surgical resection, chemotherapy, radiotherapy, targeted therapy, and immunotherapy, the clinical outcomes for CCA patients remain poor due to late diagnosis, high metastatic potential, and therapeutic resistance. This highlights the urgent need for novel molecular-targeted strategies against CCA.

Alternative mRNA splicing is a critical post-transcriptional mechanism that enables a single gene to produce multiple mRNA transcripts and protein isoforms, thereby expanding proteomic complexity. Dysregulation

of alternative splicing has been recognized as a hallmark of cancer and contributes to tumor initiation, progression, and resistance to therapy [4]. This process is tightly regulated by splicing factors, particularly the serine/arginine-rich splicing factors (SRSFs), a conserved family of 12 proteins that coordinate spliceosome assembly and splice-site selection. Aberrant expression or activity of SRSFs has been reported in multiple cancer types, leading to the generation of oncogenic splice variants and altered cellular phenotypes [5]. Abnormal alternative splicing in CCA plays a critical role by generating diverse mRNA and protein isoforms that contribute to tumor development and progression. Dysregulation of the splicing machinery and splicing factors is increasingly recognized as a key mechanism driving the aggressiveness of CCA. These alterations also represent potential therapeutic targets in CCA [6].

The activity of SRSFs is primarily regulated through phosphorylation by serine-arginine protein kinases (SRPKs). Dysregulation of the SRPK–SRSF axis has been shown to promote oncogenic splicing programs [7]. Among the 12 members of SRSFs, the upregulation of SRSF1 mRNA and protein in particular has been observed in CCA tissues and cell lines, implicating SRPK–SRSF-mediated splicing regulation in the development of CCA [8]. Pharmacological inhibition of SRPKs using small-molecule inhibitors such as SRPIN340 and SPHINX31 has demonstrated anticancer effects in several malignancies, including leukemia, melanoma, and lung cancer. These inhibitors suppress the activation of splicing factors and consequently tumor growth [7,9]. In particular, they suppress the apoptosis of CCA cells through SRSF1 phosphorylation and nuclear localization, as well as the correction of apoptotic-associated gene splicing, including *BIN1*, *MCL-1*, and *BCL2* [10]. However, inhibition of SRPK alone does not completely abolish cancer progression, indicating the activation of a possible adaptive signaling response and supporting the rationale for combination therapeutic approaches.

Proteomic profiling has emerged as a powerful strategy to identify global protein alterations and novel therapeutic targets following pathway perturbation. Components of the extracellular matrix (ECM), particularly laminin subunits, have drawn attention for their roles in cancer cell adhesion, migration, invasion, and survival. Laminin subunit beta 1 (LAMB1), a key structural component of the basement membrane, is upregulated in several cancer types and is associated with aggressive tumor behavior. Knockdown of LAMB1 significantly reduced cell proliferation, invasion, and migration in gastric cancer cells, and its expression was suppressed by the MEK inhibitor U0126 via inhibition of ERK signaling [11]. These findings suggest that LAMB1 may function downstream of oncogenic signaling pathways and serve as an adaptive survival factor following targeted inhibition. Therefore, current evidence supports further investigation of the proteomic changes induced by SRPK inhibition, as well as the exploration of rational combination strategies targeting adaptive response pathways to enhance therapeutic efficacy in CCA.

In this study, we first characterized the proteomic alterations induced by SRPK inhibition in two CCA cell lines (KKU-213A and KKU-055) using LC-MS/MS–based proteomic analysis. Second, the persistently upregulated differentially expressed proteins were identified as candidate combinatorial therapeutic targets through integration with TCGA transcriptomic data. Finally, we evaluated the antitumor efficacy of combined SRPK inhibition (SRPIN340 or SPHINX31) with a selected downstream target inhibitor (U0126) by assessing cell viability, clonogenic growth, and the associated signaling pathways involved in CCA progression.

2. Materials and Methods

2.1 Cell Lines and Cell Culture

The highly invasive cell line KKU-213A was established from a 58-year-old male and was associated with *Opisthorchis viverrini* [12]. The KKU-055 cell line was purchased from the Japanese Collection of Research Bioresources Cell Bank and was established from a poorly differentiated primary CCA tumor originating from a 56-year-old Thai male [13]. Written informed consent was obtained from all patients prior to sample collection, and the research protocol (HE621403) was approved by the Ethics Committee for Human Research of Khon Kaen University. The study was conducted in accordance with the ethical principles of the Declaration of Helsinki. KKU-213A and KKU-055 were deposited at the Japanese Collection of Research Bioresources (JCRB) Cell Bank and are available as JCRB1557 and JCRB1551, respectively. The cells were cultured in Gibco™ Dulbecco's Modified Eagle Medium (DMEM; Thermo Scientific, Waltham, MA, USA) containing 10% (v/v) Gibco™ fetal bovine serum (FBS; Thermo Scientific, Waltham, MA, USA), 100 Units/mL penicillin, and 100 µg/mL streptomycin. Cells were cultured in a humidified incubator (Thermo Scientific, Waltham, MA, USA) at 37 °C with a 5% CO_2 atmosphere. The authenticity of the cell lines was validated using Short Tandem Repeat (STR) DNA profiling. All cell lines were free of mycoplasma and were tested periodically using the Mycoalert assay (Lonza, Rockland, ME, USA).

2.2 SRPK Inhibitors and Treatments

The SRPK inhibitors SRPIN340 and SPHINX31 were purchased from Cayman Chemical Company (Ann Arbor, MI, USA). U0126 was purchased from Merck KGaA (Darmstadt, Germany). These agents were dissolved in dimethyl sulfoxide (DMSO) (Merck KGaA, Darmstadt, Germany) and stored at 4 °C. Cells were treated with various concentrations of SRPIN340, SPHINX31, or U0126 at

specified time-points, with 0.5% (v/v) DMSO used as the vehicle control (0 µM SRPIN340, SPHINX31, or U0126).

2.3 Cell Cytotoxicity and Calculation of the Inhibitory Concentration (IC)

Cell counting kit-8 (CCK-8) (Dojindo Laboratories, Kumamoto, Japan) was used to determine cell viability. Briefly, KKU-213A and KKU-055 cells were seeded in 96-well plates at 2×10^3 cells/well in complete media and incubated at 37 °C. Cells were then treated with different concentrations of SRPK inhibitors or MEK inhibitor U0126 (0.1, 1, 10, and 100 µM) for 72 h, while 0.5% (v/v) DMSO was used as the vehicle control. Subsequently, 10 µL of CCK-8 was added and the cells incubated for 4 h, followed by measurement of the absorbance at 450 nm using a microplate reader. The IC50 and IC20 values represent the concentration at which a substance exerts 50% and 20% of its maximal inhibitory effect, respectively. These were calculated with Prism 10.3.0 software (GraphPad Software, San Diego, CA, USA).

2.4 Liquid Chromatography-Tandem Mass Spectrometry (LC-MS/MS) and Protein Identification

Following treatment with 20 µM SRPIN340 or SPHINX31, total protein was extracted from KKU-213A and KKU-055 cells using radioimmunoprecipitation assay (RIPA) buffer (Thermo Fisher Scientific, Waltham, MA, USA) containing 0.05 M Tris-HCl (pH 7.4), 1% TritonX-100, 0.5% sodium deoxycholate, 0.1% SDS, 0.15 M sodium chloride, 0.002 M EDTA, and 0.05 M sodium fluoride. Total protein was measured using the Bradford assay. Each sample was adjusted to a concentration of 10 µg/µL and subjected to in-solution digestion for total proteomic analysis (Thermo Fisher Scientific, Waltham, MA, USA). The protocol for digestion and LC-MS/MS was as described in our previous study [14]. Briefly, 50 µg protein was subjected to in-solution digestion, mixed with 50 ng/µL trypsin (Promega Corporation, Madison, WI, USA), and incubated overnight at 37 °C. The digested samples were dried and protonated with 0.1% formic acid prior to LC-MS/MS. Tryptic peptide samples were prepared for injection into an Ultimate3000 Nano/Capillary LC system (Thermo Fisher Scientific, Waltham, MA, USA) coupled to a Hybrid quadrupole Q-Tof impact II™ (Bruker Daltonics, Billerica, MA, USA) equipped with a Nano-captive spray ion source. Electrospray ionization was carried out using CaptiveSpray. Mass spectra were obtained in the positive-ion mode over the range 150–2200 m/z (Compass 1.9 software; Bruker Daltonics, Billerica, MA, USA). MaxQuant software version 1.6.5.0 (Max Planck Institute of Biochemistry, Martinsried, Germany) was used to quantify the proteins, and an Andromeda search engine was employed to correlate the MS/MS spectra to the UniProt *Homo sapiens* database [15]. Only peptides with a minimum of 7 amino acids and ≥1 unique peptide were required for protein identification, and only proteins with ≥2 peptides and ≥1 unique peptide were selected for further analysis. To provide a FASTA file, all proteins present in the *Homo sapiens* proteome were downloaded from UniProt. Maximum intensities were log 2-transformed, and pairwise comparisons between control and treatment groups were performed via *t*-tests. The relationship between different sets of differentially expressed proteins was analyzed using Venn diagrams and JVENN. Visualization and statistical analyses were conducted using the MultiExperiment Viewer (MeV) in the TM4 suite software [16]. Volcano plots were used to visualize differential protein expression by integrating the magnitude of change (log 2-fold change) with statistical significance (–log 10 *p*-value). Proteins exceeding the defined thresholds were considered to be significantly different between groups.

2.5 Dataset Analysis From TCGA Database

The Cancer Genome Atlas (TCGA), an online database of human cancer, was analyzed using Gene Expression Profiling Interactive Analysis (GEPIA) (http://gepia.cancer-pku.cn/index.html), which is a communal network server. The expression profile of LAMB1 between tumor (T) and normal (N) samples in CHOL tumor types was analyzed in Transcripts-per-Million (TPM) and visualized as box-plots, while the relationship between LAMB1 expression and SRPK1 or SRPK2 expression was analyzed by correlation analysis.

2.6 RNA Extraction and Reverse Transcription Quantitative PCR (RT-qPCR)

Total RNA was extracted using RiboZol™ RNA Extraction Reagent (VWR Life Science, Radnor, PA, USA) according to the manufacturer's instructions. RNA concentration and purity were determined using a NanoDrop 2000 spectrophotometer (Thermo Fisher Scientific, Wilmington, DE, USA). Total RNA (1 µg) was reverse-transcribed into cDNA using iScript™ Reverse Transcription Supermix (Bio-Rad Laboratories, Hercules, CA, USA). Quantitative PCR (qPCR) was performed to determine LAMB1 mRNA expression. Each 20 µL reaction contained 10 ng of cDNA, 0.4 µM of each primer, and 1× HOT FIREPol® EvaGreen® qPCR Supermix (Solis BioDyne, Tartu, Estonia). The primer sequences used for LAMB1 were 5′-GAAAGCTGCCCAAAACTCCG-3′ (forward) and 5′-TTCGGCTTTCCTTCTGGCAT-3′ (reverse). The primer sequences for ACTB (β-actin) used as the internal control were 5′-GGAGGAAGGCTGGAAGAGTG-3′ (forward) and 5′-TCGTGCGTGACATTAAGGAG-3′ (reverse). Thermal cycling conditions consisted of an initial activation step at 95 °C for 12 min, followed by 40 cycles of denaturation at 95 °C for 15 s, annealing at 60 °C for 20 s, and extension at 72 °C for 20 s, with a final extension step at 72 °C for 5 min. Melt curve analysis was subsequently performed from 65 °C to 95 °C to confirm the

specificity of amplification products. All reactions were performed in triplicate. Relative gene expression levels were normalized to ACTB and calculated using the $2^{-\Delta\Delta Ct}$ method [17].

2.7 Growth Inhibition Assays

The clonogenic assay was used to determine the ability of single cells to form colonies that reflect anchorage-dependent growth in 6-well plates. The concentrations of SRPK inhibitors and U0126 used in the combination experiments were selected based on previous mechanistic evidence. SRPK inhibitors were used at 20 µM [10], whereas U0126 was used at 10 µM as a mechanistically active concentration that produced moderate inhibition while maintaining substantial cell viability. These concentrations were selected to minimize the effects of single-agent cytotoxicity while enabling evaluation of the additional inhibitory effects of combination treatment on clonogenic growth. A total of 5×10^2 KKU-213A or KKU-055 cells were seeded into 6-well plates and cultured in complete media. After 24 h, the cells were treated with 20 µM SRPIN340 or 20 µM SPHINX31 or 10 µM U0126, either alone or in combination with 10 µM U0126, for a further 24 h, while 0.5% (v/v) DMSO was used as the vehicle control. Cells were grown for 14 days, with the culture media replaced every 3 days. Colonies were fixed with 4% paraformaldehyde (Merck KGaA, Darmstadt, Germany) and then stained with 0.5% crystal violet (Sigma-Aldrich, St. Louis, MO, USA). The number, size, and density of cancer cell colonies were assessed by ImageQuant LAS500 (GE Healthcare Life Science, Amersham, UK) and analyzed by ImageQuantTL 10.2 software (GE Healthcare Life Science, Amersham, UK).

2.8 Sodium Dodecyl Sulfate-Polyacrylamide Gel Electrophoresis (SDS-PAGE) and Western Blot Analysis

KKU-213A cells were treated with 20 µM SRPIN340 or 20 µM SPHINX31, either alone or in combination with 10 µM U0126, for 24 h, while 0.5% (v/v) DMSO was used as the vehicle control. Total proteins from each treatment group were isolated using RIPA buffer containing phosphatase inhibitor (Merck Millipore, USA). Protein concentrations were measured with the Bradford assay. Equal amounts of proteins were separated by SDS-PAGE (5% stacking gel and 10% separating gel) and then transferred onto PVDF membranes (Bio-Rad Laboratories, Hercules, CA, USA). Non-specific binding was blocked with 5% skim milk (HiMedia Laboratories, Mumbai, India) and the membrane subsequently incubated overnight at 4 °C with the following specific primary antibodies: mouse anti-human p-ERK (1:10,000), mouse anti-human ERK (1:5000), mouse anti-human c-JUN (1:5000), mouse anti-human Laminin Beta-1 (1:10,000) (Santa Cruz Biotechnology, Dallas, TX, USA), or rabbit anti-human GAPDH (1:5000) (Merck Millipore, Billerica, MA, USA). This was followed by incubation with secondary antibodies: HRP-conjugated goat anti-mouse IgG (1:5000) or HRP-conjugated goat anti-rabbit IgG (1:5000) (Merck KGaA, Darmstadt, Germany). The protein bands were visualized with an Enhanced Chemiluminescence (ECL) detection system (Bio-Rad Laboratories, Hercules, CA, USA), imaged by ImageQuant LAS500 (GE Healthcare Life Science, Amersham, UK), and the signal intensities quantified using ImageJ software version 1.54 (National Institutes of Health, Bethesda, MD, USA). Protein expression was normalized to that of GAPDH as the internal control.

2.9 Statistical Analysis

Statistical analyses were performed using Prism version 10.3.0 (GraphPad Software, San Diego, CA, USA). All data are expressed as the mean ± standard deviation (SD) from triplicate biological experiments. The statistical significance of differences between multiple groups was determined with one-way ANOVA followed by Tukey's multiple comparisons *post-hoc* test where appropriate. A p-value of <0.05 was considered to indicate a statistically significant difference. Significant differences are indicated as follows in the legends: *, $^{\#}$, $^{\$} = p < 0.05$; **, $^{\#\#}$, $^{\$\$} = p < 0.01$; ***, $^{\#\#\#}$, $^{\$\$\$} = p < 0.001$.

3. Results

3.1 Effect of SRPK Inhibitors on Cell Cytotoxicity in CCA Cells

SRPK inhibition affected cell viability in a cell line-dependent manner (Fig. 1). The treatment of KKU-213A cells with SRPIN340 led to a dose-dependent reduction in cell viability, with a measurable IC20 (40.09 µM) but no IC50 achieved within the tested range (Fig. 1A). In contrast, SPHINX31 exhibited minimal cytotoxicity in this cell line, and both the IC20 and IC50 values exceeded 100 µM (Fig. 1B). SRPIN340 demonstrated a pronounced cytotoxic effect on KKU-055 cells, markedly decreasing cell viability in a dose-dependent manner with clearly defined IC50 (41.25 µM) and IC20 (20.30 µM) values (Fig. 1C). Conversely, SPHINX31 showed no significant effect on KKU-055 cell viability, with IC20 and IC50 values again exceeding the maximum tested concentration (Fig. 1D). Collectively, these findings indicate that SRPIN340 exhibits greater potency than SPHINX31 in reducing CCA cell viability, particularly in KKU-055 cells.

3.2 Proteomics Analysis of Upregulated Differentially Expressed Proteins (UpDEPs)

The UpDEPs in SRPK inhibitor-treated CCA cells (KKU-213A and KKU-055) were identified using LC–MS/MS and analyzed with computational bioinformatics approaches. A total of 814 and 695 UpDEPs were detected in SRPIN340- and SPHINX31-treated KKU-213A cells, respectively, while 1,037 and 864 UpDEPs were identified in SRPIN340- and SPHINX31-treated KKU-055 cells. Venn

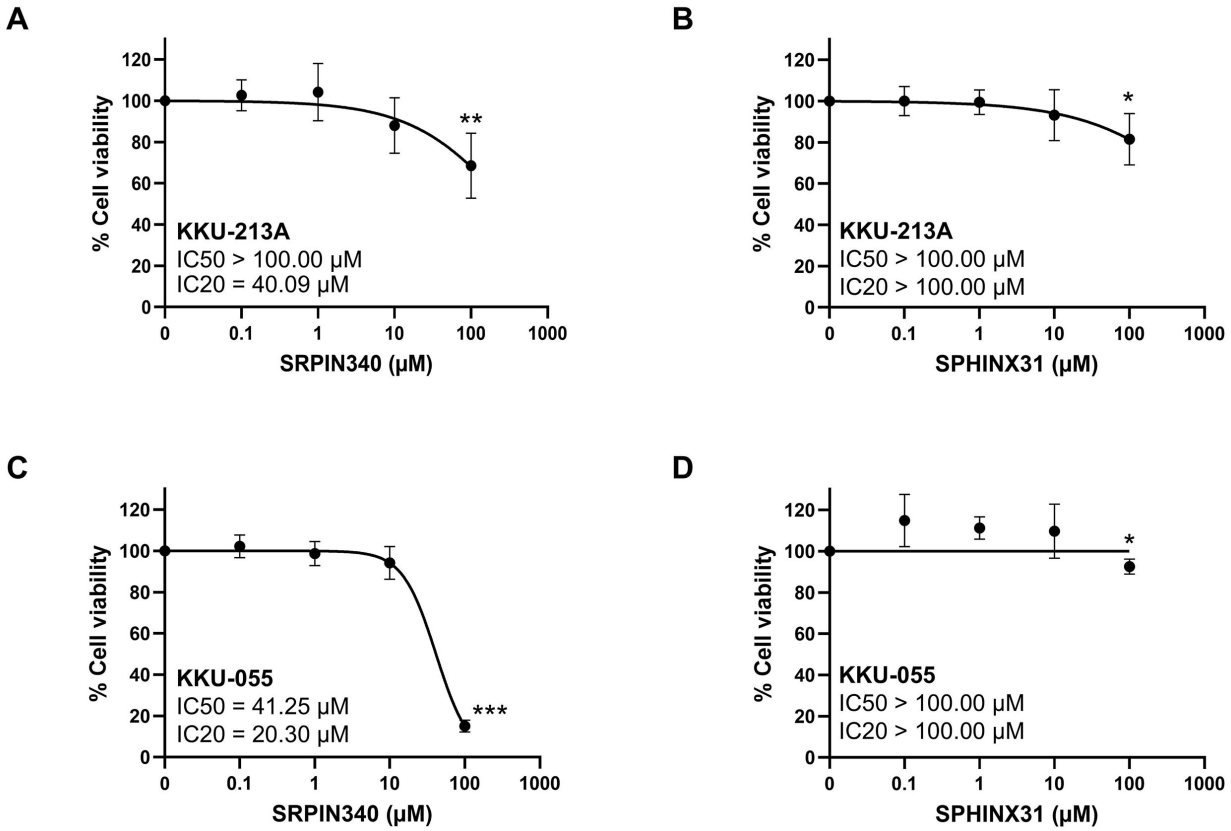

Fig. 1. Effects of SRPK inhibitors on CCA cell viability. The viability of CCA cell lines (KKU-213A and KKU-055) following treatment with SRPK inhibitors, SRPIN340 and SPHINX31, was assessed by CCK-8 assay in KKU-213A cells (A,B) and KKU-055 cells (C,D). In KKU-213A cells, SRPIN340 reduced cell viability more effectively than SPHINX31. The IC50 and IC20 values are indicated in each panel, but the values >100.00 μM represent the highest tested concentration at which 50% or 20% inhibition was not achieved. Data are presented as mean ± SD from triplicate biological experiments, and statistical significance is indicated (*$p < 0.05$, **$p < 0.01$, ***$p < 0.001$). SRPK, serine-arginine protein kinase; CCA, cholangiocarcinoma; CCK-8, cell counting kit-8.

diagram analysis revealed 363 and 500 commonly upregulated proteins (log 2-fold change ≥1.00) in KKU-213A and KKU-055 cells, respectively (Fig. 2A). Notably, 34 UpDEPs were shared between both cell lines. These common UpDEPs were further visualized using a heatmap, the proteins included in the heatmaps had already been selected based on the predefined differential expression criteria described in the Methods. The heatmaps were therefore intended to visualize the expression patterns of these selected proteins rather than to present their individual statistical values. The heatmap of the top 20 proteins ranked based on SRPIN340-treatment in each CCA cell line (Fig. 2B). Furthermore, volcano plot analysis of the 34 shared UpDEPs in KKU-213A (Fig. 2C) and KKU-055 (Fig. 2D) confirmed the significant upregulation of LAMB1, suggesting a consistent response to SRPK inhibition across both cell lines.

3.3 Selection of a Candidate Combinatorial Target for SRPK Inhibition in CCA Cells

LAMB1 was selected based on multiple complementary criteria rather than differential expression alone. First, LAMB1 showed consistent upregulation in response to both SRPK inhibitors (SRPIN340 and SPHINX31) across both CCA cell lines (KKU-213A and KKU-055). In contrast, although several other UpDEPs showed higher fold changes when the protein list was sorted according to SRPIN340 treatment (Fig. 2B), they were not selected as candidate combinatorial targets because their responses were less consistent across cell lines or inhibitors. Specifically, SLTP004 and aconitase 2 (ACO2) exhibited cell-specific responses, with markedly higher fold changes in KKU-213A cells but lower fold changes in KKU-055 cells. Similarly, GRM2 showed an inhibitor-specific response, with a pronounced increase following SRPIN340 treatment but a lower fold change following SPHINX31 treatment. Second, the concurrent upregulation of another laminin family member (LAMC1), suggesting coordinated regulation of laminin-associated pathways. Third, its therapeutic potential as a druggable target supported by previous studies reporting that available inhibitors can suppress its expression [11].

Analysis of TCGA CHOL datasets revealed that LAMB1 was significantly upregulated in tumor tissues (T)

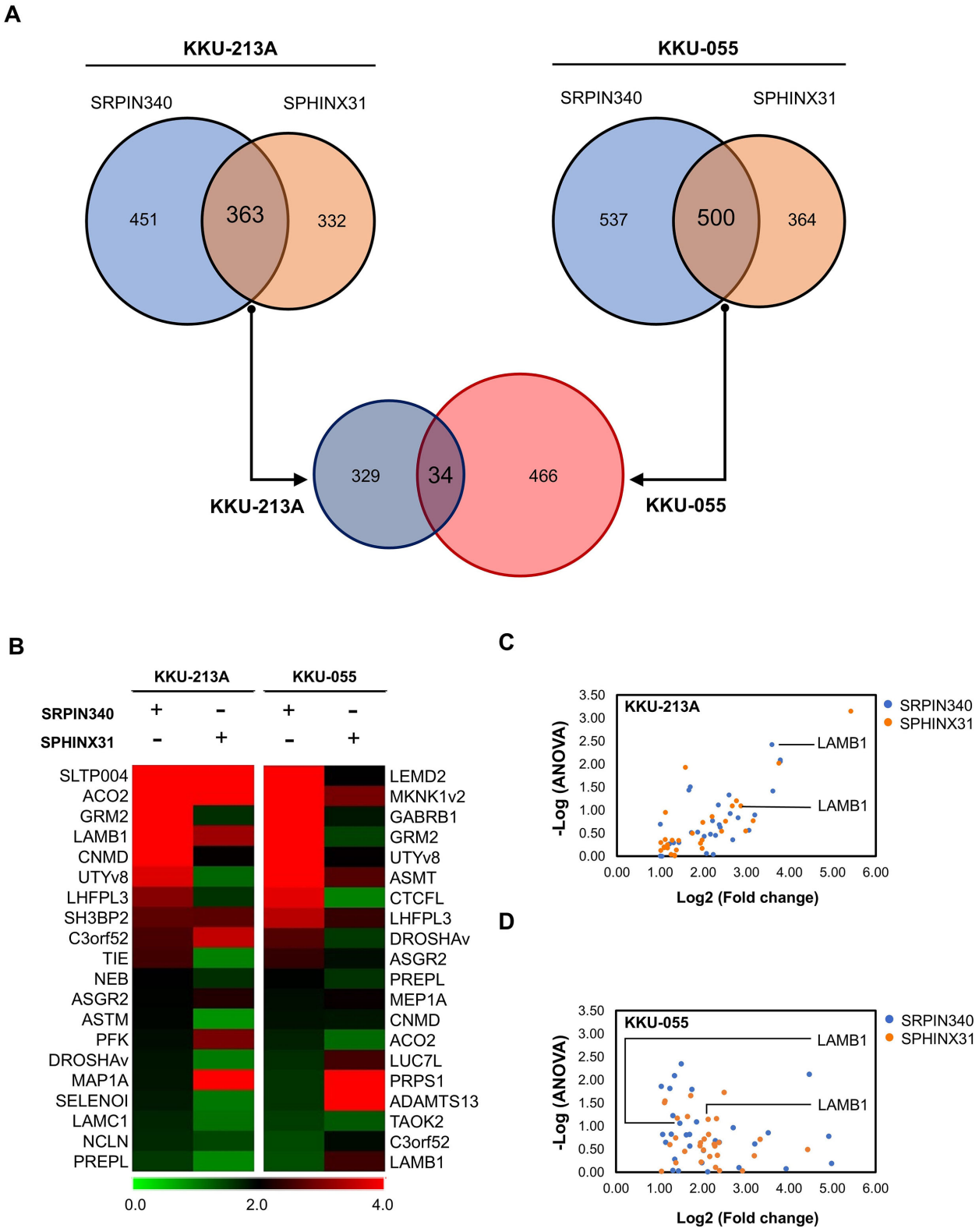

Fig. 2. Proteomic analysis of upregulated-differentially expressed proteins (UpDEPs) in CCA cells following SRPK inhibitor treatment. Venn diagrams showing overlapping upregulated proteins in KKU-213A and KKU-055 cells treated with SRPIN340 or SPHINX31 (log 2 fold change ≥1.00) (A). Common UpDEPs between treatments and cell lines are indicated, Heatmap of the top 20 UpDEPs shared between KKU-213A and KKU-055, ranked based on SRPIN340-treatment (B). Volcano plots of UpDEPs highlighting significantly altered proteins, including LAMB1 in KKU-213A cells (C) and KKU-055 cells (D).

compared to normal controls (N) (Fig. 3A). Furthermore, RT-qPCR confirmed the upregulation of LAMB1 mRNA following SRPIN340 and SPHINX31 treatment in both KKU-213A (Fig. 3B) and KKU-055 (Fig. 3C) cells, although statistical significance was only observed in KKU-213A cells. Based on these findings, LAMB1 was selected as a candidate combinatorial target for SRPK inhibition.

3.4 Effect of MEK Inhibition by U0126 on SRPK Inhibitor-Induced LAMB1-Associated Growth Suppression in CCA Cells

We next explored a potential combinatorial strategy by combining SRPK inhibition with MEK inhibition. U0126, a selective MEK inhibitor, has been reported to modulate LAMB1 expression in other cancer models [11]. Based on these findings, we investigated whether combining U0126 with SRPK inhibitors could further enhance the anti-proliferative effects in CCA cells. U0126 treatment reduced cell viability in both KKU-213A and KKU-055 cells, as determined by CCK-8 assay (Fig. 3D,E). A clear dose-dependent effect was observed in KKU-213A cells with a measurable IC20 (1.60 μM), but no IC50 was achieved within the tested range (Fig. 3D). KKU-055 cells also exhibited marked sensitivity at higher concentrations, with clearly defined IC50 (47.18 μM) and IC20 (24.38 μM) values (Fig. 3E). These results support the potential of MEK inhibition as a complementary approach for modulating LAMB1-associated pathways in CCA.

3.5 Evaluation of the Combinatorial Effects of SRPK and LAMB1 Inhibition on CCA Cell Viability

The effects of both SRPK inhibitors and the MEK inhibitor-U0126 on KKU-213A cells were evaluated alone and in combination. SRPIN340 or U0126 alone modestly reduced cell viability, while their combination (SRPIN340 + U0126) markedly reduced cell viability compared with either single treatment (Fig. 4A). In contrast, SPHINX31 or U0126 alone showed minimal effects, whereas their combination (SPHINX31 + U0126) significantly decreased cell viability (Fig. 4B). Similarly, SRPIN340 or U0126 alone reduced the viability of KKU-055 cells, but their combined treatment further enhanced the cytotoxic effect (Fig. 4C). Although SPHINX31 or U0126 alone had limited impact, their combination significantly suppressed cell viability (Fig. 4D).

Collectively, these findings demonstrate that co-targeting of the SRPK and MEK pathways enhances the inhibitory effects on CCA cell viability compared with treatment by single agents.

3.6 Evaluation of the Combinatorial Effects of SRPK and MEK Inhibition on CCA Cell Growth

Clonogenic assays were performed to assess long-term cell growth following treatment with SRPIN340, SPHINX31, and their combination with U0126. Neither single nor combined treatments of KKU-213A cells significantly affected the total number of colonies (Fig. 5A,B). However, combination treatments, particularly SPHINX31 + U0126, markedly reduced the number of large colonies (>500 pixels with was predefined before image analysis and applied identically to all experimental groups to ensure consistency), indicating impaired colony growth capacity (Fig. 5C).

The colonies of KKU-055 cells were generally smaller in size after 14 days compared with KKU-213A cells (Fig. 5D), and neither single nor combined treatments significantly altered the total colony number or the number of large colonies (Fig. 5E,F). These results suggest that the combinatorial effect was more pronounced in KKU-213A cells, whereas no statistically significant enhancement was observed in KKU-055 cells under the experimental conditions used.

3.7 Evaluation of Combined SRPK and MEK Inhibition on LAMB1-Associated Signaling in KKU-213A Cells

Given the pronounced growth-inhibitory effects observed in KKU-213A cells, this cell line was selected for the mechanistic analysis of LAMB1-related signaling. The effects of SRPK inhibitors (alone or in combination with the MEK inhibitor U0126) on key upstream regulatory proteins of LAMB1 were examined by Western blotting. Specifically, the expression levels of phosphorylated ERK (p-ERK), total ERK, and the transcription factor cellular Jun proto-oncogene (c-JUN) were assessed, along with LAMB1 protein levels. Band intensities were quantified and normalized to the untreated control (set as 1.00), and the p-ERK/ERK ratio was calculated to evaluate ERK pathway activation.

Single treatment with SRPIN340 or SPHINX31 increased p-ERK levels. Specifically, treatment with SRPIN340 alone also increased c-JUN and LAMB1 levels. This observation is consistent with the proteomic findings that identified LAMB1 as an upregulated protein following SRPK inhibition. In contrast, co-treatment with U0126 markedly reduced p-ERK levels and decreased the p-ERK/ERK ratio, confirming effective suppression of ERK activation. This was accompanied by a reduction in c-JUN and LAMB1 protein expression, suggesting that ERK signaling may be involved in the regulation of LAMB1 expression (Fig. 6).

The above results indicate that SRPK inhibition alone may activate ERK signaling, leading to increased LAMB1 expression, whereas combined inhibition with SRPK and MEK effectively suppresses this pathway. This mechanistic evidence supports the stronger inhibitory effects of combination observed in cell viability and clonogenic assays.

4. Discussion

Aberrant alternative splicing is increasingly recognized as a hallmark of cancer [18] and has been implicated in the development and progression of CCA [6]. In

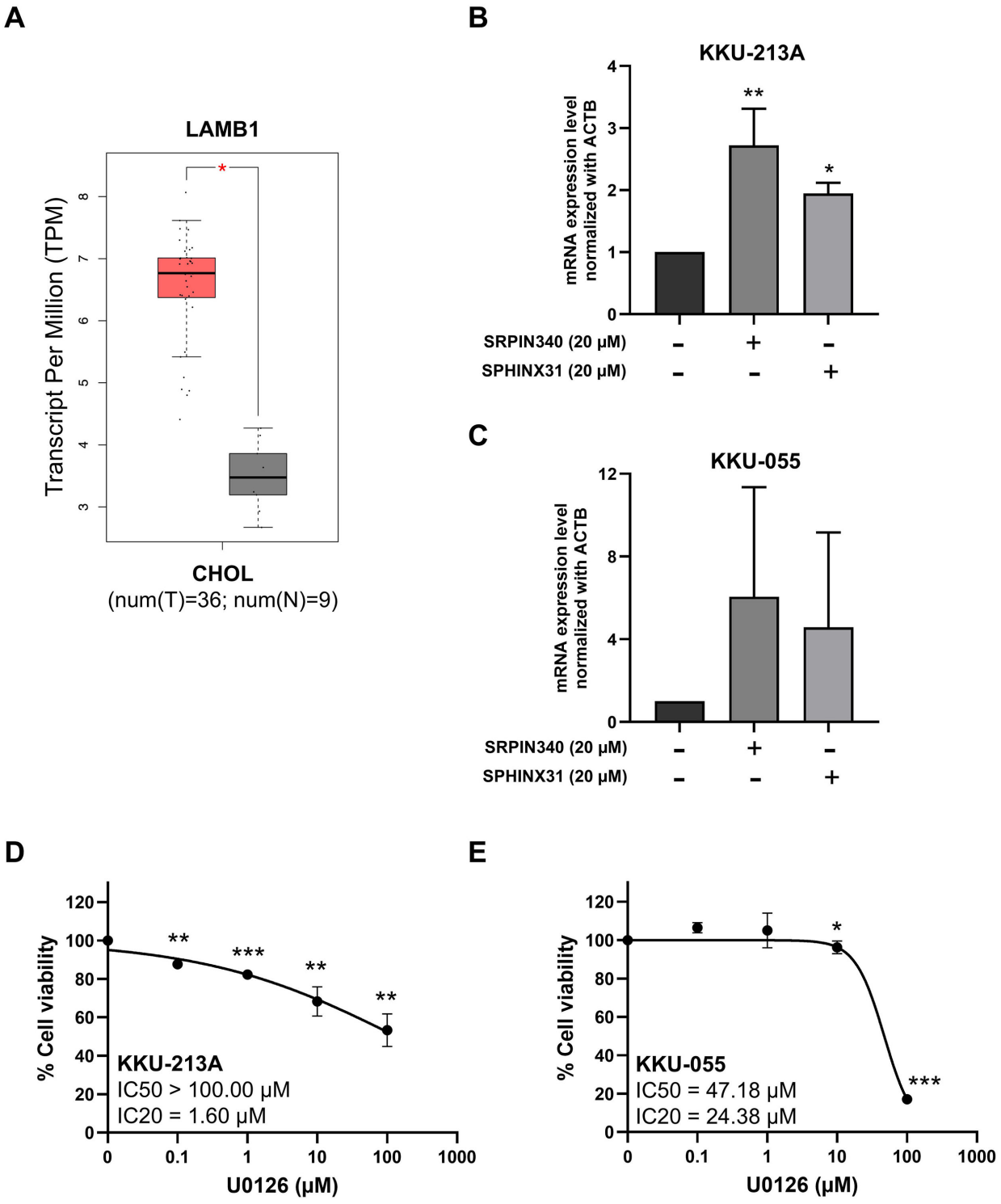

Fig. 3. Selection of LAMB1 as a candidate combinatorial target and effects of MEK inhibitor-U0126 on CCA cell viability. Box plot showing LAMB1 mRNA expression in cholangiocarcinoma (CHOL) tumor tissues (T) compared with normal tissues (N) from TCGA datasets (A). RT-qPCR validation of LAMB1 mRNA levels in KKU-213A (B) and KKU-055 (C) cells treated with SRPIN340 or SPHINX31. Effects of MEK inhibitor-U0126 on cell viability in KKU-213A (D) and KKU-055 (E) cells, determined by CCK-8 assay. U0126 reduced cell viability in a dose-dependent manner, with IC50 and IC20 values indicated in each panel. Data are presented as mean ± SD, and statistical significance is indicated (*$p < 0.05$, **$p < 0.01$, ***$p < 0.001$).

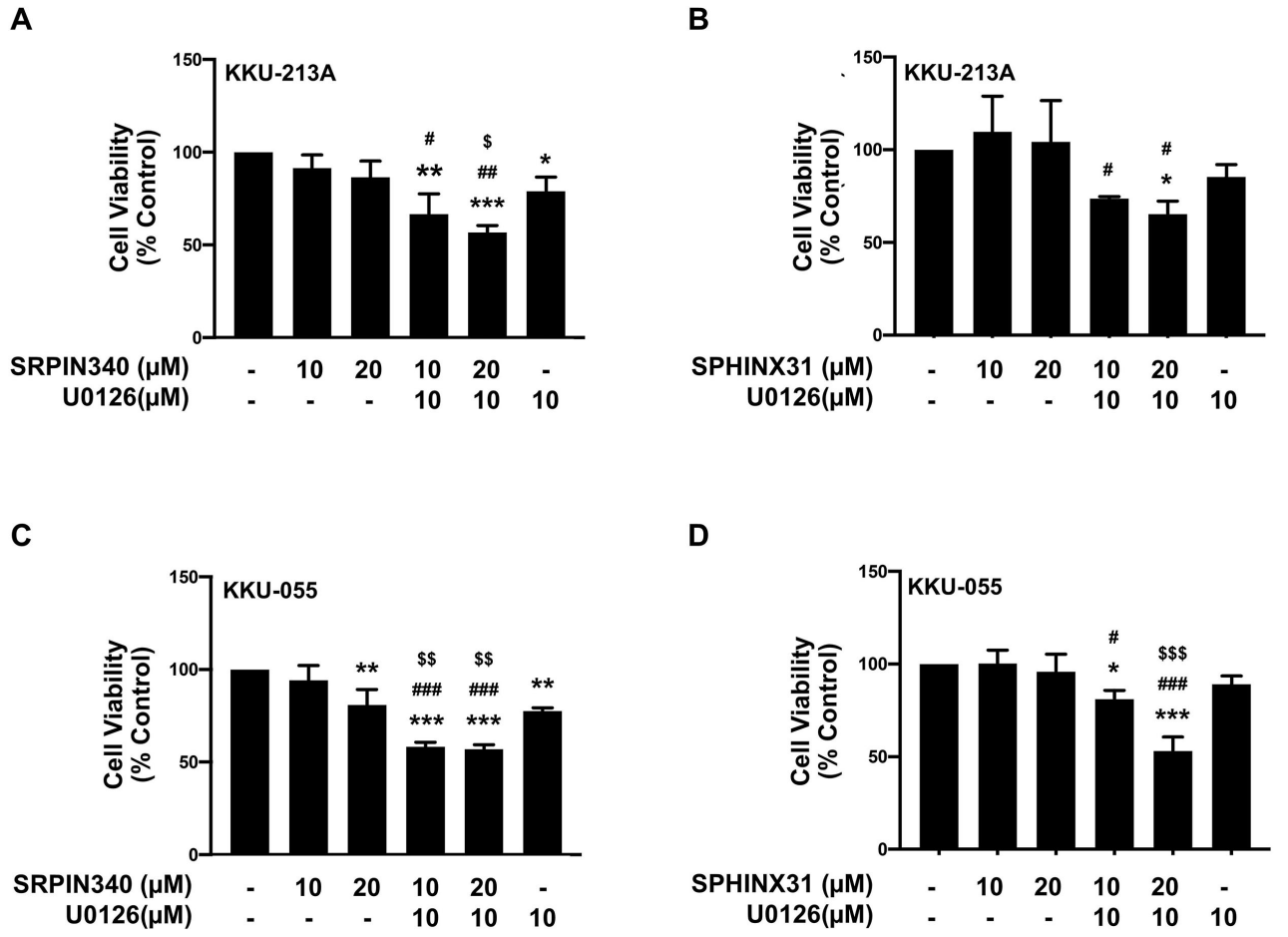

Fig. 4. Effects of SRPK inhibitors and MEK inhibitors on CCA cell viability. Cell viability of KKU-213A cells treated with SRPIN340 (A) or SPHINX31 (B), alone or in combination with U0126. Cell viability of KKU-055 cells treated with SRPIN340 (C) or SPHINX31 (D), alone or in combination with U0126. Cell viability was measured by CCK-8 assay and expressed as a percentage of control. Data are presented as mean ± SD, and statistical significance is indicated (*; compared with control, #; compared with SRPK inhibitor and $; compared with U0126), *, #, $ = $p < 0.05$, **, ##, $$ = $p < 0.01$ and ***, ###, $$$ = $p < 0.001$.

the present study, we targeted upstream regulators of alternative splicing by inhibiting SRPK activity using two compounds, SRPIN340 and SPHINX31, to suppress downstream splicing mechanisms. SRPIN340 has been reported to inhibit melanoma xenograft growth [19], and to induce apoptosis in CCA cells [10]. Similarly, the SRPK1-specific inhibitor SPHINX31 reduces the clonogenic growth and migration of melanoma cells [20], and also induces apoptosis in CCA cells [10]. Although previous studies have shown that both inhibitors reduce the viability of CCA cells, their effects are incomplete, highlighting the need for improved or combinatorial therapeutic strategies.

Previous studies have investigated splicing kinase inhibitors that target both SRPKs and CDC-like kinases (CLKs), including CPD-1, CPD-2, and CPD-3. These inhibitors showed stronger growth suppressive effects (GI50 at 72 h) than SRPIN340 and SPHINX31 in breast, non-small cell lung, and colorectal cancer cell lines [21]. However, the CPD compounds lack specificity, as they inhibit both SRPK and CLK families. In contrast, SRPIN340 and SPHINX31 selectively target SRPK function, making them more suitable for evaluating SRPK-specific mechanisms.

In the current study, SRPK inhibition by SRPIN340 and SPHINX31 induced distinct cytotoxic responses in KKU-213A and KKU-055 cells. It was previously reported that SRPIN340 exhibits moderate activity in leukemia cell lines, with IC50 values ranging from approximately 44.7 to 92.2 μM [7]. In contrast, SPHINX31 showed higher potency, with IC50 values of 0.19 μM in THP1 cells, 0.27 μM in NOMO-1 cells, 8.37 μM in HL60 cells, and 13.23 μM in HEL cells [22]. SPHINX31 was also evaluated in melanoma cells, although IC50 values were not clearly defined under the tested conditions [20]. Our results showed that SRPIN340 exhibited measurable cytotoxicity in KKU-055 cells, with a definable IC50 value, whereas the IC50 value could not be determined in KKU-213A cells within

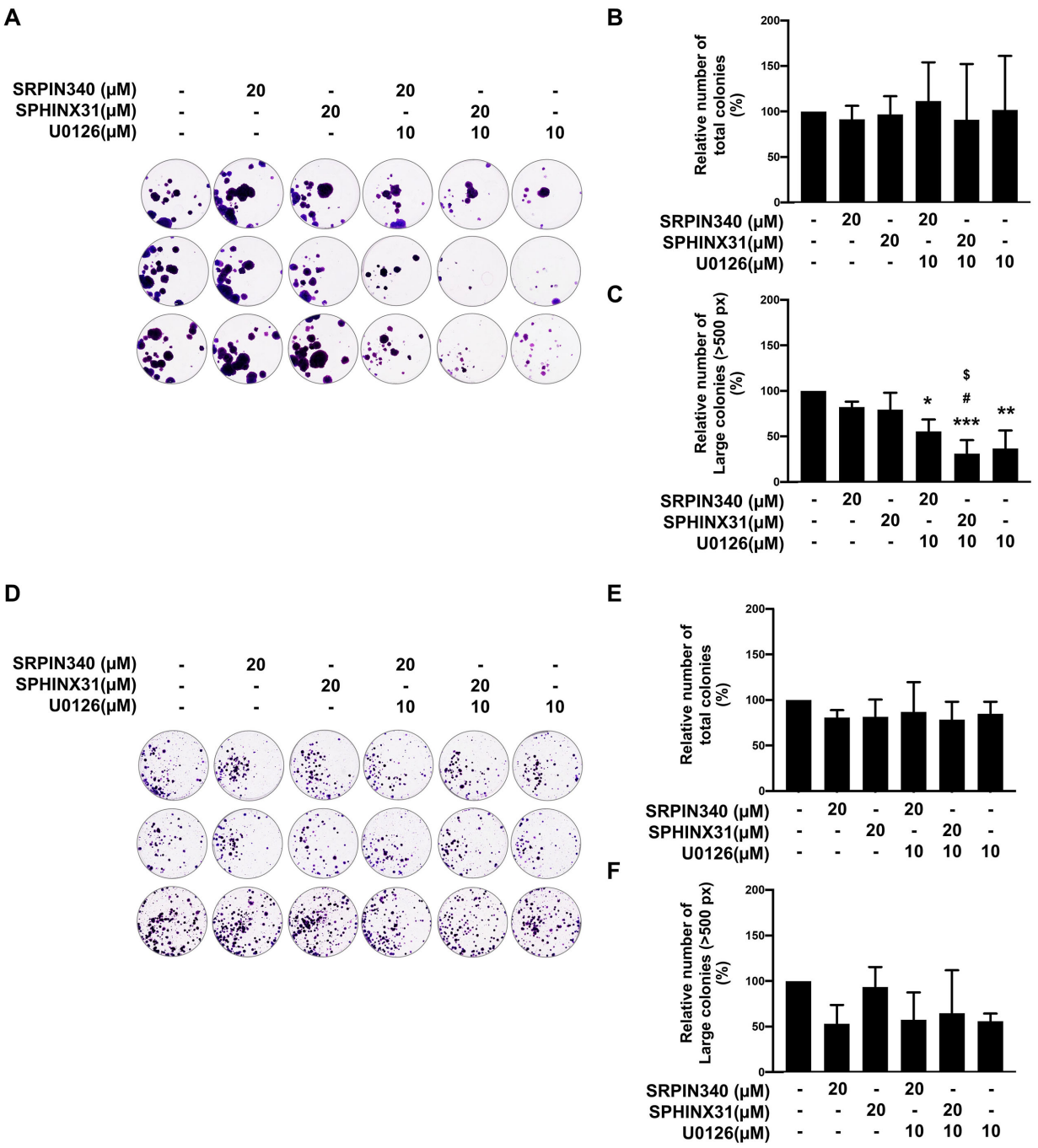

Fig. 5. Effects of SRPK inhibitors and MEK inhibitors on clonogenic growth of CCA cells. Representative images of colony formation in KKU-213A (A) and KKU-055 (D) cells treated with SRPIN340 or SPHINX31, alone or in combination with U0126, followed by crystal violet staining. Quantification of the relative total number of colonies (B,E). Quantification of the relative number of large colonies (>500 pixels) (C,F). Data are presented as mean ± SD, and statistical significance is indicated (*; compared with control, #; compared with SRPK inhibitor and $; compared with U0126), *, #, $ = $p < 0.05$, ** = $p < 0.01$ and *** = $p < 0.001$.

the tested concentration range (Fig. 1A,C). Similarly, the IC50 values for SPHINX31 could not be determined in either KKU-213A or KKU-055 cells within the tested concentration range (Fig. 1B,D). Higher concentrations could not be evaluated due to the precipitation of SPHINX31 in DMSO, which restricted its solubility and prevented accurate assessment of its full inhibitory potential. However, the incomplete suppression of cell viability observed with SRPK inhibitors alone suggests that additional combinatorial strategies are required to enhance their therapeutic efficacy.

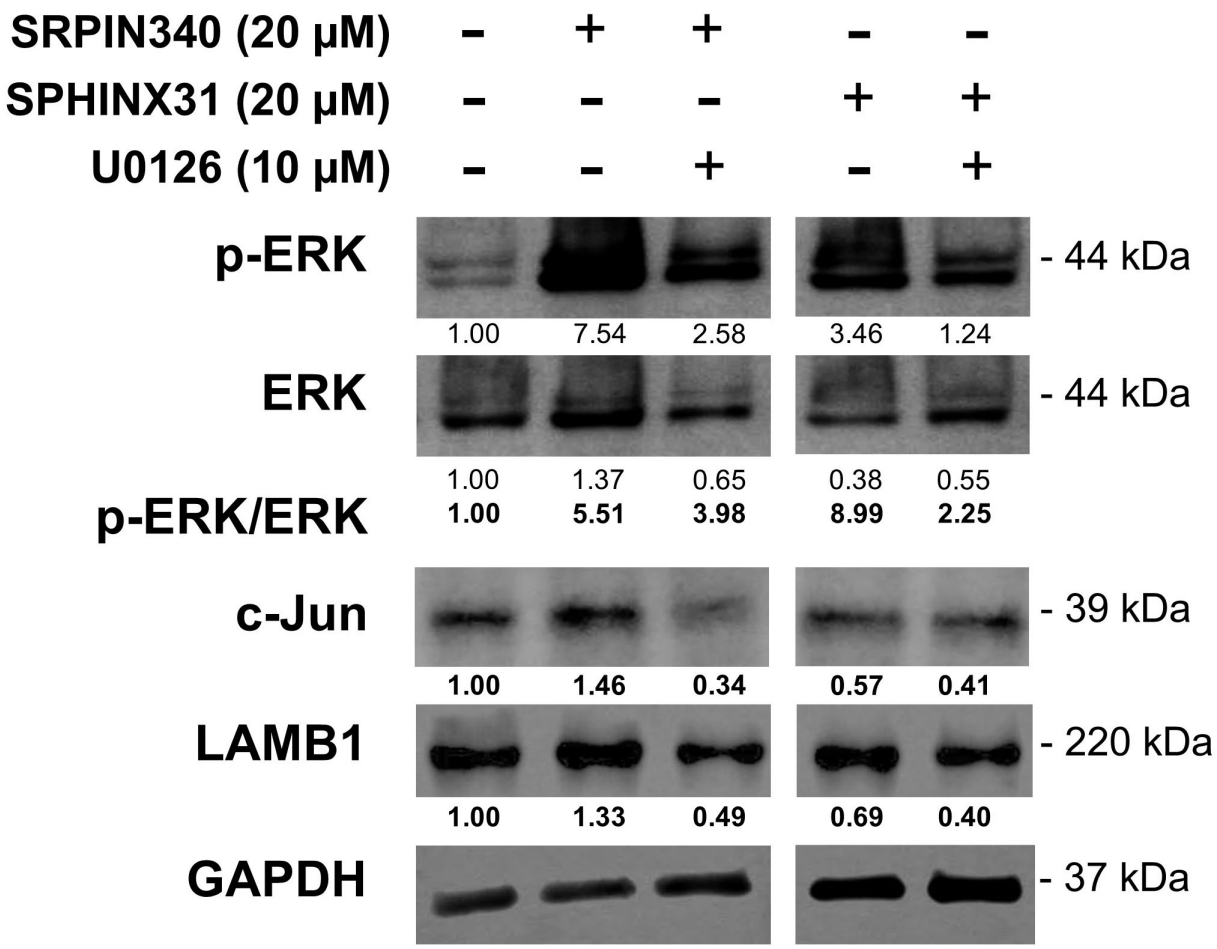

Fig. 6. Effects of SRPK inhibitors and MEK inhibitors on LAMB1-associated signaling in KKU-213A cells. KKU-213A cells were treated with SRPIN340 or SPHINX31 (20 μM), alone or in combination with the MEK inhibitor U0126 (10 μM), as indicated. Protein expression levels of phosphorylated ERK (p-ERK), total ERK, c-JUN, and LAMB1 were analyzed by western blotting, with GAPDH used as a loading control. Relative band intensities (normalized to control, set as 1.00) are shown below each protein band. The ratio of p-ERK to ERK (p-ERK/ERK) is also presented to indicate ERK activation status. Molecular weights (kDa) are indicated on the right.

To enhance the efficacy of growth inhibition in CCA, previous studies have applied proteomic approaches to identify possible adaptive mechanisms following targeted therapy. For example, proteomic analysis of LAT1 inhibitor-treated CCA cells (targeting the L-type amino acid transporter 1 protein) revealed upregulation of cell cycle-related proteins. This was subsequently used to guide the selection of cell cycle inhibitors for combination treatment [23]. In line with this strategy, we performed proteomic profiling of CCA cells treated with the SRPK inhibitor to identify potential adaptive responses. Our analysis identified a subset of UpDEPs, including 34 proteins commonly upregulated by both SRPK inhibitors (SRPIN340 and SPHINX31) and in both CCA cell lines (KKU-213A and KKU-055) (Fig. 2A). These shared UpDEPs may represent candidate targets for rational combination strategies to improve therapeutic outcomes.

To identify candidate targets for combination therapy, we performed heatmap and volcano plot analyses on the proteomic dataset. Among the commonly upregulated proteins, LAMB1 was consistently and significantly increased in response to both SRPK inhibitors and across both CCA cell lines (Fig. 2B,C). To further validate its relevance, LAMB1 expression was examined at the mRNA level in TPM-counts using GEPIA analysis of TCGA CCA datasets [24]. This analysis confirmed significant upregulation in tumor tissues compared with normal controls (Fig. 3A). Consistent with the proteomic findings, RT-qPCR analysis further confirmed that SRPIN340 and SPHINX31 treatment significantly increased LAMB1 mRNA expression in KKU-213A cells, with a similar increasing trend observed in KKU-055 cells (Fig. 3B,C). Together, these findings provide strong evidence supporting LAMB1 as a biologically relevant and rational candidate for combination targeting following SRPK inhibition.

Recent studies have consistently demonstrated that LAMB1 functions as a pro-tumorigenic ECM protein involved in cancer progression. In nasopharyngeal carcinoma, LAMB1 was shown to promote tumor cell proliferation, migration, and invasion, while also shaping an immune-suppressive tumor microenvironment by reducing T-cell infiltration and immune activation [25]. A recent study in hepatocellular carcinoma (HCC) found that LAMB1 is frequently upregulated and promotes tumor growth, invasion, and metastasis through activation of integrin-mediated signaling pathways such as focal adhesion kinase (FAK)/proto-oncogene tyrosine-protein kinase Src (SRC)/yes-associated protein 1 (YAP1). Functionally, LAMB1 enhances cell proliferation and contributes to tumor aggressiveness and poor prognosis [26]. Emerging evidence indicates that LAMB1 is significantly overexpressed in CCA and is associated with ECM remodeling, cell migration, and drug resistance [27]. Functional studies suggest that LAMB1 promotes malignant phenotypes and chemoresistance, while the suppression of LAMB1 reduces tumor aggressiveness [28]. Laminin-integrin interactions, including LAMB1-containing complexes, also play a key role in enhancing CCA cell migration and metastatic potential [29]. Overall, accumulating evidence supports LAMB1 as a critical regulator of tumor growth, metastasis, and immune modulation, highlighting its potential as a therapeutic target and biomarker across multiple cancer types, including CCA.

In the present study, LAMB1 was identified as a candidate combinatorial target, based on the hypothesis that CCA cells may survive SRPK inhibition through LAMB1-mediated adaptive response mechanisms. A key limitation has been the lack of a specific LAMB1 inhibitor. However, a previous study in gastric cancer reported that MEK inhibition by U0126 reduced LAMB1 expression through inhibition of ERK phosphorylation and subsequent suppression of c-Jun-mediated transcription. Whether this mechanism is conserved in CCA remains to be determined [11]. Therefore, U0126 was employed in the current study as an indirect approach for modulating LAMB1-associated signaling in CCA cells. Our results showed that combined treatment with SRPK inhibitors and U0126 significantly reduced CCA cell proliferation compared with single-agent treatments (SRPIN340, SPHINX31, or U0126), supporting a greater inhibitory effects of the combined treatment (Fig. 4). This finding is consistent with a previous study in CCA, where U0126 enhanced the inhibitory effect of TGF-β1 on cell viability [30]. Moreover, in colorectal cancer, U0126 was found to synergize with chemotherapeutic agents such as oxaliplatin and 5-fluorouracil (5-FU) [31]. Collectively, these results support the rationale for combining SRPK and MEK inhibition to overcome adaptive survival pathways mediated by LAMB1.

The effects of combined SRPK and U0126 on long-term cell growth were also evaluated using a clonogenic assay. The combination of SRPK inhibitors with U0126 did not significantly alter the total number of colonies of either KKU-213A cells (Fig. 5A,B) or KKU-055 cells (Fig. 5D,E). However, a marked reduction in the number of large colonies was observed in KKU-213A cells (Fig. 5C), indicating the combination treatment preferentially suppresses colony expansion rather than the initial formation of colonies. This observation suggests that combined inhibition by SRPK and MEK may impair cell proliferative capacity and colony growth dynamics. In line with this, a previous study showed that U0126 reduces colony formation, invasion, and migration of gastric cancer cells [11]. U0126 has also been reported to synergize with TGF-β1 in CCA cells, resulting in a greater reduction in colony area compared with single treatments [30]. Together, these findings support the role of MEK inhibition in limiting tumor growth, while reinforcing its potential in combination strategies.

Based on the results of cell viability and clonogenic assays, the combination of SRPK inhibitors with U0126 exerted a more pronounced inhibitory effect on KKU-213A cells than on KKU-055 cells. This differential response may reflect the intrinsic molecular and pharmacological heterogeneity of CCA cell lines. Consistent with this possibility, comprehensive drug-response profiling showed that KKU-213A exhibited greater sensitivity to MEK inhibitors than KKU-055 [32]. However, the molecular basis underlying this differential response was not investigated in the present study. Therefore, KKU-213A cells were selected for further mechanistic investigation of LAMB1-associated signaling. Western blot analysis was performed to evaluate the effects of SRPK inhibitors (alone or in combination with U0126) on the expression of key regulatory proteins, including p-ERK/ERK, c-JUN, and LAMB1 (Fig. 6). Treatment with SRPIN340 or SPHINX31 alone increased the expression of p-ERK, c-JUN, and LAMB1, consistent with the proteomic findings indicating that inhibition of SRPK upregulates LAMB1. In contrast, combined treatment with U0126 markedly reduced the expression of p-ERK, c-JUN, and LAMB1, suggesting effective suppression of ERK signaling and its downstream transcriptional regulation. These molecular changes are consistent with the observed reductions in cell viability and colony growth. Notably, similar effects have been reported in gastric cancer, where U0126 suppressed p-ERK, c-JUN, and LAMB1 expression [11], thereby suggesting a possible involvement of the ERK/c-Jun signaling pathway in LAMB1 regulation; however, the underlying mechanism requires further experimental validation.

In summary, inhibition of SRPK alone is limited by adaptive LAMB1 upregulation, whereas combined SRPK and MEK inhibition effectively suppresses CCA cell growth through modulation of the ERK/c-JUN/LAMB1 axis. These findings highlight a potential combination strategy that warrants further investigation.

The main limitations of the present study, including: (i) the use of only two established cholangiocarcinoma cell lines without validation in additional cell lines or patient-derived models; (ii) the absence of *in vivo* validation to evaluate the therapeutic efficacy of the proposed combination strategy; (iii) the lack of genetic and rescue experiments to establish a direct causal role of the ERK/c-JUN/LAMB1 signaling axis; (iv) the use of SRPK inhibitors and U0126 at concentrations that did not produce equivalent levels of single-agent inhibition, which prevents clear determination of the relative contribution of each inhibitor to the combined effect and (v) the absence of formal drug synergy analysis using the combination index (CI) using the Chou–Talalay method, together with isobologram analysis.

5. Conclusions

SRPK inhibition alone is insufficient to fully suppress the progression of CCA, as adaptive response mechanisms such as LAMB1 upregulation may limit its efficacy. This study identified LAMB1 as a potential downstream target associated with SRPK activity, and also demonstrated that combined inhibition of SRPK (using SRPIN340 or SPHINX31) and MEK signaling (using U0126) enhances antitumor effects. The combination of SRPK inhibitors with U0126 resulted in greater inhibition of cell viability and clonogenic growth than either treatment alone, and was accompanied by suppression of ERK and c-JUN signaling. These findings suggest that dual targeting of the SRPK and MEK pathways represents a promising therapeutic strategy for improving treatment outcomes in CCA.

Abbreviations

5-FU, 5-fluorouracil; ACO2, aconitase 2; ANOVA, analysis of variance; CCA/CHOL, cholangiocarcinoma; CCK-8, cell counting kit-8; CLKs, CDC-like kinases; c-JUN, cellular Jun proto-oncogene; DMEM, Dulbecco's modified Eagle medium; DMSO, dimethyl sulfoxide; ECL, enhanced chemiluminescence; ECM, extracellular matrix; EDTA, ethylene-diamine-tetraacetic acid; ERK, extracellular signal-regulated kinase; FAK, focal adhesion kinase; FBS, fetal bovine serum; GAPDH, glyceraldehyde-3-phosphate dehydrogenase; GEPIA, Gene Expression Profiling Interactive Analysis; GRM2, glutamate metabotropic receptor 2; HCC, hepatocellular carcinoma; HCl, hydrochloric acid; HRP, horseradish peroxidase; IC, inhibitory concentration; IgG, immunoglobulin G; JCRB, the Japanese Collection of Research Bioresources; JVENN, JavaScript Venn; LAMC1, laminin subunit gamma 1; LAMB1, Laminin subunit beta 1; LAT1, L-type amino acid transporter 1; LC-MS/MS, liquid chromatography-tandem mass spectrometry; MEK, mitogen-activated protein kinase kinase; MeV, multiple experiment viewer; mRNA, messenger Ribonucleic Acid; N, normal tissues; PAGE, polyacrylamide gel electrophoresis; p-ERK, phosphorylated extracellular signal-regulated kinase; RIPA, radioimmunoprecipitation assay; SD, standard deviation; SDS, sodium dodecyl sulfate; SLTP004, uncharacterized protein SLTP004; SRC, proto-oncogene tyrosine-protein kinase Src; SRPK1, serine-arginine protein kinase 1; SRPK2, serine-arginine protein kinase 2; SRPKs, serine-arginine protein kinases; SRSF1, serine/arginine rich-splicing factor 1; SRSFs, serine/arginine rich-splicing factors; STR, short tandem repeat; T, tumor tissues; TCGA, The Cancer Genome Atlas; TGF-β1, transforming growth factor beta 1; TPM, Transcript per million; UpDEPs, upregulated differentially expressed proteins; WB, Western blotting; YAP1, yes-associated protein 1.

Availability of Data and Materials

The raw data and all other datasets analyzed during the current study are available from the corresponding author on reasonable request.

Author Contributions

CI, TJ, AS, SR and WK conceived and designed the work; CI, PK, PV, HI and WK curated data: CI, PK, PV, WS, KK and SR performed the experiments; CI, PK, HI, SR and WK analyzed the data; CI, PK and WK wrote the manuscript; TJ, AS, SR and WK administrated project; TV, HI, AS, SR and WK supervised; All authors read and approved the final manuscript. All authors contributed to editorial changes in the manuscript. All authors have participated sufficiently in the work and agreed to be accountable for all aspects of the work.

Ethics Approval and Consent to Participate

Written informed consent was obtained from all patients prior to sample collection, and the research protocol (HE621403) was approved by the Ethics Committee for Human Research of Khon Kaen University. The study was conducted in accordance with the ethical principles of the Declaration of Helsinki.

Acknowledgment

Not applicable.

Funding

This study was supported by the grant from National Research Council of Thailand (NRCT), NRCT-Research Career Development Grant (Grant NO. NRCT5-RSA63011-04) to Worasak Kaewkong. In addition, the part of proteomics and data analysis was supported by NRCT, the Royal Golden Jubilee (RGJ) Ph.D. Programme (Contact No. N41A680262) to Chaturong Inpad.

Conflicts of Interest

The authors declare no conflicts of interest.

References

[1] Kodali S, Shetty A, Shekhar S, Victor DW, Ghobrial RM. Management of Intrahepatic Cholangiocarcinoma. Journal of Clinical Medicine. 2021; 10: 2368. https://doi.org/10.3390/jcm10112368

[2] Banales JM, Marin JJG, Lamarca A, Rodrigues PM, Khan SA, Roberts LR, et al. Cholangiocarcinoma 2020: the next horizon in mechanisms and management. Nature Reviews. Gastroenterology & Hepatology. 2020; 17: 557–588. https://doi.org/10.1038/s41575-020-0310-z

[3] Banales JM, Rodrigues PM, Affò S, Andersen JB, Aspichueta P, Boulter L, et al. Cholangiocarcinoma 2026: status quo, unmet needs and priorities. Nature Reviews. Gastroenterology & Hepatology. 2026; 23: 65–96. https://doi.org/10.1038/s41575-025-01153-w

[4] da Silva MR, Moreira GA, Silva RA, Barbosa E, Pais SR, Teixeira RR, et al. Splicing regulators and their roles in cancer biology and therapy. BioMed Research International. 2015; 2015: 1–12. https://doi.org/10.1155/2015/150514

[5] Zhou X, Li X, Yu L, Wang R, Hua D, Shi C, et al. The RNA-binding protein SRSF1 is a key cell cycle regulator via stabilizing NEAT1 in glioma. The International Journal of Biochemistry & Cell Biology. 2019; 113: 75–86. https://doi.org/10.1016/j.biocel.2019.06.003

[6] Marin JJG, Reviejo M, Soto M, Lozano E, Asensio M, Ortiz-Rivero S, et al. Impact of Alternative Splicing Variants on Liver Cancer Biology. Cancers. 2021; 14: 18. https://doi.org/10.3390/cancers14010018

[7] Siqueira RP, Barbosa ÉDAA, Polêto MD, Righetto GL, Seraphim TV, Salgado RL, et al. Potential Antileukemia Effect and Structural Analyses of SRPK Inhibition by N-(2-(Piperidin-1-yl)-5-(Trifluoromethyl)Phenyl)Isonicotinamide (SRPIN340). PloS One. 2015; 10: e0134882. https://doi.org/10.1371/journal.pone.0134882

[8] Inpad C, Phetchahwang P, Pothipan P, Tangwiriyarotkul P, Hongsrichan N, Horpaopan S, et al. Silencing serine/arginine-rich splicing factor 1 to induce apoptosis and autophagy-dependent cell death in cholangiocarcinoma through the correction of oncogenic splicing errors. Anatomy & Cell Biology. 2025; 58: 602–614. https://doi.org/10.5115/acb.25.052

[9] Supradit K, Boonsri B, Duangdara J, Thitiphatphuvanon T, Suriyonplengsaeng C, Kangsamaksin T, et al. Inhibition of serine/arginine-rich protein kinase-1 (SRPK1) prevents cholangiocarcinoma cells induced angiogenesis. Toxicology In Vitro. 2022; 82: 105385. https://doi.org/10.1016/j.tiv.2022.105385

[10] Changphasuk P, Inpad C, Horpaopan S, Khunchai S, Phimsen S, Surangkul D, et al. SRPK Inhibitors Reduce the Phosphorylation and Translocation of SR Protein Splicing Factors, thereby Correcting *BIN1*, *MCL-1* and *BCL2* Splicing Errors and Enabling Apoptosis of Cholangiocarcinoma Cells. Frontiers in Bioscience (Scholar Edition). 2024; 16: 17. https://doi.org/10.31083/j.fbs1603017

[11] Lee H, Kim WJ, Kang HG, Jang JH, Choi IJ, Chun KH, et al. Upregulation of LAMB1 via ERK/c-Jun Axis Promotes Gastric Cancer Growth and Motility. International Journal of Molecular Sciences. 2021; 22: 626. https://doi.org/10.3390/ijms22020626

[12] Sripa B, Seubwai W, Vaeteewoottacharn K, Sawanyawisuth K, Silsirivanit A, Kaewkong W, et al. Functional and genetic characterization of three cell lines derived from a single tumor of an Opisthorchis viverrini-associated cholangiocarcinoma patient. Human Cell. 2020; 33: 695–708. https://doi.org/10.1007/s13577-020-00334-w

[13] Panawan O, Silsirivanit A, Chang CH, Putthisen S, Boonnate P, Yokota T, et al. Establishment and characterization of a novel cancer stem-like cell of cholangiocarcinoma. Cancer Science. 2023; 114: 3230–3246. https://doi.org/10.1111/cas.15812

[14] Pratummanee K, Kerdkumthong K, Roytrakul S, Tantimetta P, Runsaeng P, Saeheng S, et al. Knockdown of cullin 3 inhibits progressive phenotypes and increases chemosensitivity in cholangiocarcinoma cells. Molecular Medicine Reports. 2024; 30: 198. https://doi.org/10.3892/mmr.2024.13322

[15] Tyanova S, Temu T, Cox J. The MaxQuant computational platform for mass spectrometry-based shotgun proteomics. Nature Protocols. 2016; 11: 2301–2319. https://doi.org/10.1038/nprot.2016.136

[16] Howe EA, Sinha R, Schlauch D, Quackenbush J. RNA-Seq analysis in MeV. Bioinformatics (Oxford, England). 2011; 27: 3209–3210. https://doi.org/10.1093/bioinformatics/btr490

[17] Livak KJ, Schmittgen TD. Analysis of relative gene expression data using real-time quantitative PCR and the 2(-Delta Delta C(T)) Method. Methods (San Diego, Calif.). 2001; 25: 402–408. https://doi.org/10.1006/meth.2001.1262

[18] Ladomery M. Aberrant alternative splicing is another hallmark of cancer. International Journal of Cell Biology. 2013; 2013: 463786. https://doi.org/10.1155/2013/463786

[19] Gammons MV, Lucas R, Dean R, Coupland SE, Oltean S, Bates DO. Targeting SRPK1 to control VEGF-mediated tumour angiogenesis in metastatic melanoma. British Journal of Cancer. 2014; 111: 477–485. https://doi.org/10.1038/bjc.2014.342

[20] Siriwath J, Wiriyakulsit N, Klomkleang P, Inpad C, Roytrakul S, Kaewkong W. SPHINX31 suppresses splicing factor phosphorylation and inhibits melanoma cell growth and aggressiveness. Journal of Current Science and Technology. 2021; 11: 346–354

[21] Araki S, Dairiki R, Nakayama Y, Murai A, Miyashita R, Iwatani M, et al. Inhibitors of CLK protein kinases suppress cell growth and induce apoptosis by modulating pre-mRNA splicing. PloS One. 2015; 10: e0116929. https://doi.org/10.1371/journal.pone.0116929

[22] Tzelepis K, De Braekeleer E, Aspris D, Barbieri I, Vijayabaskar MS, Liu WH, et al. SRPK1 maintains acute myeloid leukemia through effects on isoform usage of epigenetic regulators including BRD4. Nature Communications. 2018; 9: 5378. https://doi.org/10.1038/s41467-018-07620-0

[23] Okanishi H, Ohgaki R, Okuda S, Endou H, Kanai Y. Proteomics and phosphoproteomics reveal key regulators associated with cytostatic effect of amino acid transporter LAT1 inhibitor. Cancer Science. 2021; 112: 871–883. https://doi.org/10.1111/cas.14756

[24] Farshidfar F, Zheng S, Gingras MC, Newton Y, Shih J, Robertson AG, et al. Integrative Genomic Analysis of Cholangiocarcinoma Identifies Distinct IDH-Mutant Molecular Profiles. Cell Reports. 2017; 18: 2780–2794. https://doi.org/10.1016/j.celrep.2017.02.033

[25] Feng E, Yang X, Yang J, Qu Q, Li X. LAMB1 promotes proliferation and metastasis in nasopharyngeal carcinoma and shapes the immune-suppressive tumor microenvironment. Brazilian Journal of Otorhinolaryngology. 2025; 91: 101551. https://doi.org/10.1016/j.bjorl.2024.101551

[26] Cai Z, Li J, Wu L, Hu X, Lin W, Peng B, et al. Laminin β1 stimulates the Hippo-YAP1 pathway to advance the progression and lenvatinib resistance in hepatocellular carcinoma. International Journal of Biological Macromolecules. 2026; 336: 149150. https://doi.org/10.1016/j.ijbiomac.2025.149150

[27] Tantimetta P, Chaimeteveth N, Nounsuwan K, Urairat C, Yongpraderm D, Rattanaarchanai T, et al. TCGA and bioinformatics reveal the molecular network and prognostic implication of Laminin beta 1 in cholangiocarcinoma. Current Applied Science And Technology. 2025; 2025: e0267583. https://doi.org/10.55003/cast.2025.267583

[28] Kerdkumthong K, Roytrakul S, Songsurin K, Pratummanee K, Runsaeng P, Obchoei S. Proteomics and Bioinformatics Identify Drug-Resistant-Related Genes with Prognostic Potential in

Cholangiocarcinoma. Biomolecules. 2024; 14: 969. https://doi.org/10.3390/biom14080969

[29] Islam K, Thummarati P, Kaewkong P, Sripa B, Suthiphongchai T. Role of laminin and cognate receptors in cholangiocarcinoma cell migration. Cell Adhesion & Migration. 2021; 15: 152–165. https://doi.org/10.1080/19336918.2021.1924422

[30] Sritananuwat P, Sueangoen N, Thummarati P, Islam K, Suthiphongchai T. Blocking ERK1/2 signaling impairs TGF-β1 tumor promoting function but enhances its tumor suppressing role in intrahepatic cholangiocarcinoma cells. Cancer Cell International. 2017; 17: 85. https://doi.org/10.1186/s12935-017-0454-2

[31] Jing C, Li H, Du Y, Cao H, Liu S, Wang Z, et al. MEK inhibitor enhanced the antitumor effect of oxaliplatin and 5-fluorouracil in MEK1 Q56P-mutant colorectal cancer cells. Molecular Medicine Reports. 2019; 19: 1092–1100. https://doi.org/10.3892/mmr.2018.9730

[32] Jamnongsong S, Kueanjinda P, Buraphat P, Sakornsakolpat P, Vaeteewoottacharn K, Okada S, et al. Comprehensive drug response profiling and pan-omic analysis identified therapeutic candidates and prognostic biomarkers for Asian cholangiocarcinoma. iscience. 2022; 25: 105182. https://doi.org/10.1016/j.isci.2022.105182